CHARMS IN RELATIVISTIC HEAVY-ION COLLISIONS* **

Che Ming Ko[a], Su Houng Lee[b], Wei Liu[a], Yongseok Oh[c]
Shigehiro Yasui[d], Ben-Wei Zhang[e]

[a]Cyclotron Institute and Department of Physics and Astronomy
Texas A&M University, College Station
Texas 77843-3366, USA
[b]Institute of Physics and Applied Physics, Yonsei University, Seoul 120-749, Korea
[c]Korea Institute of Science and Technology Information, Daejeon 305-806, Korea
[d]High Energy Accelerator Research Organization (KEK)
Tsukuba, Ibaraki, 302-0801, Japan
[e]Institute of Particle Physics, Central China Normal University
Wuhan 430079, China

(Received January 27, 2010)

Studying charm production in relativistic heavy-ion collisions provides the possibility to probe the properties of produced quark–gluon plasma. In this paper, we review our work on charm quark energy loss, charmed baryon to meson ratio, thermal charm production, and the production of charmed multiquark hadrons in relativistic heavy-ion collisions.

PACS numbers: 25.75.–q, 25.75.Cj, 25.75.Dw

1. Introduction

Studying the production of hadrons consisting of heavy charm quarks is a topic of great interest in relativistic heavy-ion collisions. This includes charmonium suppression as a possible signature for the Quark–Gluon Plasma (QGP) [1], the charm elliptic flow and quenching as a probe of the charm quark interactions in QGP [2–4], and the production of exotic charmed tetraquark and pentaquark hadrons [5, 6]. In this paper, we review our work on charm quark energy loss [7], charmed baryon to meson ratio [8, 9], thermal charm production [10], and the production of charmed multiquark

* Talk presented at the EMMI Workshop and XXVI Max Born Symposium "Three Days of Strong Interactions", Wrocław, Poland, July 9–11, 2009.

** Supported by the U.S. National Science Foundation under Grant No. PHY-0758115 and the Welch Foundation under Grant No. A-1358.

hadrons [6] in relativistic heavy-ion collisions. For charm quark energy loss in QGP, the contribution of charm quark three-body scattering is found to be non-negligible. For charmed baryon production, we have found in the quark coalescence model that it is significantly enhanced in heavy-ion collisions at RHIC than in proton–proton collisions, particularly if strong diquark correlations exist in QGP. For thermal charm production, a next-to-leading order calculation shows that it could be appreciably enhanced in heavy-ion collisions at LHC as a result of the high temperature that is expected to be reached in the produced QGP. For charmed multiquark hadrons, which are likely to exist due to the color–spin interaction in diquarks, we have estimated their yields in relativistic heavy-ion collisions using the quark coalescence model.

2. Charm quark energy loss

Studying charm quark energy loss offers the possibility to understand both the interaction of charm quarks in QGP and the properties of QGP. Experimentally, electrons from semi-lepton decays of charmed and bottomed hadrons have been measured at RHIC [11, 12]. Their suppression at high transverse momentum was found to be as large as that for light hadrons and could not be explained by radiative energy loss of heavy quarks in QGP. Additional energy loss of heavy quarks due to two-body elastic scattering has thus been suggested [13, 14]. This effect is further enhanced if colorless resonances are formed in charm quark scattering with light antiquarks [15]. Also, heavy quarks can lose energy as a result of collisional dissociation of heavy mesons resulting from their fragmentations inside the QGP [16]. Since the density of the partonic matter formed in heavy-ion collisions at RHIC is large, ranging from about 1 fm^{-3} near hadronization to more than 10 fm^{-3} during the initial stage, three-body scattering may also contribute to heavy quark energy loss in QGP. In Ref. [7], we have studied this effect.

For heavy quark elastic scattering with two light quarks or antiquarks of different flavors, there are three topologically different diagrams in the lowest-order QCD. Its momentum degradation in a QGP then depends on the drag coefficient $\gamma(|\boldsymbol{p}|,T) = \sum_i \left(\langle\overline{|\mathcal{M}_i|^2}\rangle - \langle\overline{|\mathcal{M}_i|^2}\boldsymbol{p}\cdot\boldsymbol{p}'\rangle/|\boldsymbol{p}|^2\right)$, where $\boldsymbol{p}$ and $\boldsymbol{p}'$ are, respectively, momenta of the heavy quark before and after a collision. The sum is over all scattering processes with $\overline{|\mathcal{M}_i|^2}$ being their squared amplitudes after averaging over the spins and colors of initial partons and summing over those of final partons. The symbol $\langle\cdots\rangle$ denotes average over the thermal distributions of scattered partons in the QGP and integration over the momenta of all final-state partons. Using the screening mass $m_D = gT$ for space-like gluons, the thermal masses $m_q = m_g/\sqrt{3} = m_D/\sqrt{6}$ for time-like light quarks and gluons, and the

QCD coupling $\alpha_s = g^2/4\pi = 0.3$, we have found that heavy quark drag coefficients in QGP due to these three-body processes are dominated by t-channel gluon exchange diagrams. For other three-body elastic scattering processes of heavy quarks by quarks and/or antiquarks with same flavors or by gluons, we have assumed that they are also dominated by similar diagrams. In the left window of Fig. 1, charm (upper panels) and bottom (lower panels) quark drag coefficients due to all three-body elastic scattering processes are shown by dash-dotted lines as functions of their momentum in QGP at temperatures $T = 200$ and 300 MeV. Compared to drag coefficients due to two-body elastic and radiative scatterings, which we have also calculated from respective lowest order Born diagrams, the drag coefficient from three-body elastic scattering is comparable to that from two-body elastic scattering (dotted lines), and both are more important than that due to radiative scatterings (dashed lines) if the momentum of a charm quark is below about 4 GeV/c and that of a bottom quark is below about 9 GeV/c.

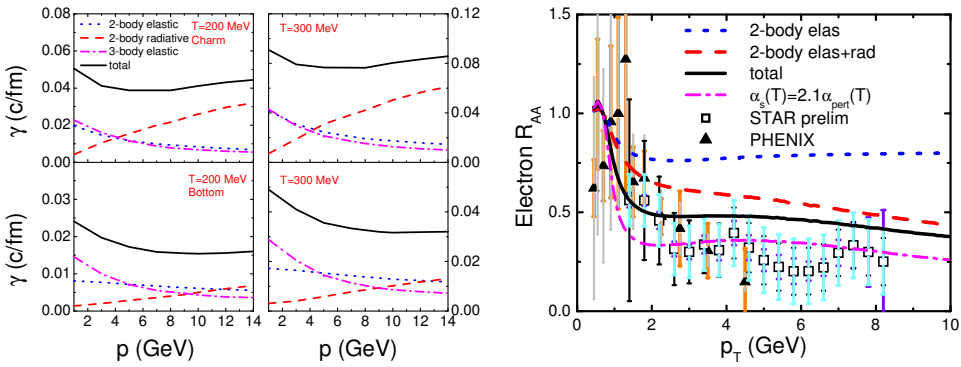

Fig. 1. (Color online) Left panels: Charm and bottom quark drag coefficients as functions of their momentuum in a QGP of temperature $T = 200$ or $T = 300$ MeV. Right panel: Nuclear modification factor R_{AA} for electrons from heavy quark decays in central Au + Au collisions at $\sqrt{s_{NN}} = 200$ GeV.

In an expanding fireball model, we have studied the momentum degradation of midrapidity heavy quarks in the QGP produced in central Au + Au collisions at center-of-mass energy $\sqrt{s_{NN}} = 200$ GeV. The initial heavy quark transverse momentum p_T spectra are obtained from those of p+p collisions at same energy multiplied by the number of binary collisions (~ 960) in Au + Au collisions. For $p + p$ collisions, the charm quark p_T spectrum is determined from fitting the STAR charmed meson data for d+Au collisions [17] using the Peterson fragmentation function $D(z) \sim 1/(z[1-1/z-\epsilon/(1-z)]^2)$ with $\epsilon = 0.02$ for the charm quark, while that of bottom quarks is taken from the pQCD predictions [18]. The p_T spectrum of electrons from decays of resulting heavy charmed and bottomed mesons, with the latter obtained

from bottom quarks using $\epsilon = 0.002$ in the Peterson fragmentation function, reproduces the measured one by the STAR collaboration for $p + p$ collisions. Neglecting the dispersion of heavy quark transverse momentum with respect to their mean values, which is the case for high transverse momentum heavy quarks, the time evolution of the mean transverse momentum $\langle p_{\rm T}\rangle$ of a heavy quark in QGP is then approximately given by $d\langle p_{\rm T}\rangle/dt \approx -\gamma(\langle p_{\rm T}\rangle, T)\langle p_{\rm T}\rangle$. The heavy quark is fragmented into mesons when it leaves the QGP or until the end of the QGP stage if it remains inside. The resulting electron nuclear modification factor R_{AA}, defined as the ratio of the electron $p_{\rm T}$ spectrum from decays of final heavy mesons to that from initially produced ones, is shown in the right window of Fig. 1. It is seen that including contributions from both two-body elastic and radiative scattering gives an electron R_{AA} (dashed line) that is about a factor of two smaller than that due to two-body elastic scattering alone (dotted line), similar to that found in Ref. [14] and still significantly above the experimental data from the PHENIX (filled triangles) [11] and STAR (open squares) [12] collaborations. Adding contributions from heavy quark three-body elastic scattering further reduces the electron R_{AA} (solid line). Since studies based on both hydrodynamic [19] and transport [20] models have indicated that the large elliptic flow observed in heavy-ion collisions at RHIC is consistent with a produced QGP that is strongly coupled, *i.e.*, it has a small viscosity or involves large parton scattering cross-section. This is further supported by results from lattice QCD studies that the QCD coupling constant at temperatures achieved at RHIC is larger than that from the perturbative QCD, *i.e.*, $\alpha_{\rm s}(T) = g^2(T)/4\pi \approx 2.1\alpha_{\rm pert}(T)$ [21]. Using this enhanced strong coupling constant, we have recalculated heavy quark drag coefficients. The resulting electron R_{AA} from heavy meson decays in Au + Au collisions at $\sqrt{s_{NN}} = 200$ GeV are shown in the right window of Fig. 1 by the dash-dotted line and are seen to reproduce reasonably the experimental data.

3. Charmed baryon to meson ratio

Another interesting phenomena in heavy-ion collisions at RHIC is the possible enhancement of the ratios of heavy baryons to heavy mesons, especially if strong diquark (ud) correlations exist in the quark–gluon plasma [8]. The existence of diquark correlations in QGP can be probed by studying their effects on Λ_c production in relativistic heavy-ion collisions. Using the quark coalescence model, we have recently studied the Λ_c/D^0 and $\Lambda_b/\bar{B}^0$ ratios in heavy-ion collisions by including also the resonance decay effects [9]. For the width parameters of hadron Wigner functions used in the coalescence model, they are determined by requiring that the majority of heavy hadrons

at low p_{T} are formed from coalescence, and the remaining heavy quarks are then converted to heavy hadrons via fragmentation as in pp collisions. For central Au + Au collisions at $\sqrt{s_{NN}} = 200$ GeV, the Λ_c/D^0 ratio is found to be 1.34, which is about 10.3 larger than the prediction of the PYTHIA model, and about a factor of 5.0 larger than that of the thermal model. The enhancement of the Λ_c/D^0 ratio due to diquarks is about 1.6. For the transverse momentum dependence of the Λ_c/D^0 ratio, we have found that it peaks at $p_{\mathrm{T}} \simeq 2$ GeV in the three-quark model and at $p_{\mathrm{T}} \simeq 0.8$ GeV in the diquark model as shown in the left window of Fig. 2. Therefore, the enhancement of charmed baryon production over charmed meson production due to diquarks can mostly be observed at low p_{T} region. These results are based on a diquark mass of 445 MeV or a binding energy of 145 MeV. Because of the thermal factor, the number of diquarks decreases as the diquark mass increases, and this would reduce Λ_c production and increase that of D^0, reducing thus the Λ_c/D^0 ratio. For example, if the diquark mass is 550 MeV, the enhancement of the Λ_c/D^0 ratio due to diquarks would reduce from 1.6 to 1.3. The peak position in the ratio changes, however, very little. Similar results are obtained for Λ_b and $\bar{B}^0$ and their ratio as shown in the right window of Fig. 2. The enhanced Λ_c/D^0 ratio, which is expected to suppress the electron R_{AA} as the branching ratio of Λ_c decay into electrons is smaller than that of D^0, does not lead, however, to additional suppression of the electron R_{AA} at large transverse momenta (≥ 5 GeV) [22], where the suppression is mainly due to heavy quark energy loss in produced quark–gluon plasma.

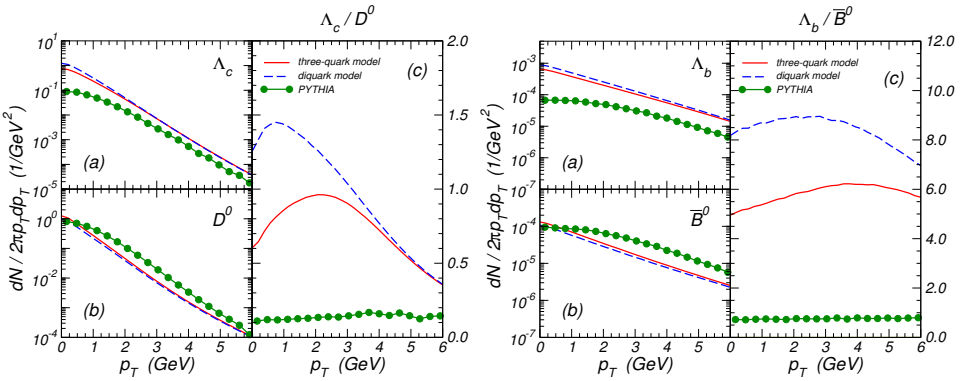

Fig. 2. Left window: spectra of (a) Λ_c and (b) D^0, and (c) the ratio Λ_c/D^0 in midrapidity ($|y| \leq 0.5$) for central Au + Au collisions at $\sqrt{s_{NN}} = 200$ GeV. Solid lines are for the three-quark model and dashed lines are for the diquark model. Results from the PYTHIA model are shown by filled circles. Right window: same for bottomed hadrons.

4. Thermal charm production

Charm quark production from the quark–gluon plasma formed in relativistic heavy-ion collisions was previously studied in Ref. [23] based on gluon fusions in the leading-order QCD. Compared to the number of charm quarks produced from initial hard scattering between incident nucleons, this study shows that the number of thermally produced charm quarks is negligible unless the temperature of the quark–gluon plasma is very high. We have re-examined this problem in the next-to-leading order in QCD [10]. Specifically, we have included the processes $q+\bar{q} \to c+\bar{c}$ and $g+g \to c+\bar{c}$ and their virtual corrections as well as the processes $q+\bar{q} \to c+\bar{c}+g$ and $g+g \to c+\bar{c}+g$. The amplitudes for these processes were taken from Refs. [24,25] using massless quarks and gluons, the QCD coupling constant $\alpha_s(m_c) \approx 0.37$, and a charm quark mass $m_c = 1.3$ GeV. The charm quark production rate in the quark–gluon plasma was then evaluated by integrating over the thermal quark and gluon distributions in the quark–gluon plasma, which are taken to have masses $m_g = \sqrt{3}m_q = gT/\sqrt{2}$ with T being the temperature of the quark–gluon plasma and g related to the thermal QCD coupling constant $\alpha_s(2\pi T) = g^2/4\pi$ of values ranging from ~ 0.23 for $T = 700\,\mathrm{MeV}$ to ~ 0.42 for $T = 170\,\mathrm{MeV}$. For both quark–antiquark annihilation and gluon–gluon fusion, charm quark pair production cross-sections and their thermal averages are larger in the next-to-leading order than in the leading order and depend sensitively on the temperature of the quark–gluon plasma. In the left window of Fig. 3, we show the temperature dependence of the charm quark pair production rates per unit volume from the leading order (dashed line) and the next-to-leading order (solid line). Both are appreciable at high temperatures with the latter larger than the former, and their ratio varies from ~ 4.5 at low temperatures to ~ 1.8 at high temperatures as shown in the inset in the figure. Since the initial temperature achieved in heavy-ion collisions at RHIC is only about 350 MeV, thermal charm quark production is thus unimportant.

This is different in heavy-ion collisions at LHC where the initial temperature of the formed quark–gluon plasma is expected to be much higher. To estimate the contribution of thermal charm quark production in central Pb + Pb collisions $\sqrt{s_{NN}} = 5.5$ TeV at LHC, we model the dynamics of formed quark–gluon plasma by assuming that it evolves boost invariantly in the longitudinal direction but with an accelerated transverse expansion. Specifically, its volume expands in the proper time τ according to $V(\tau) = \pi R^2(\tau)\tau c$, where $R(\tau) = R_0 + a(\tau - \tau_0)^2/2$ is the transverse radius with an initial value $R_0 = 7$ fm, the quark–gluon plasma formation time τ_0, and the transverse acceleration $a = 0.1\ c^2/\mathrm{fm}$. Starting with an initial temperature $T_0 = 700\,\mathrm{MeV}$ at $\tau_0 = 0.2\ \mathrm{fm}/c$, the time dependence of the temperature is obtained from entropy conservation, leading to the critical

temperature $T_{\rm C} = 170\,{\rm MeV}$ at proper time $\tau_{\rm C} = 6.4\ {\rm fm}/c$. The initial number of charm pairs is taken to be $dN_{c\bar{c}}/dy = 20$ at midrapidity, which is of similar magnitude as that estimated from initial hard nucleon–nucleon collisions based on the next-to-leading order pQCD calculations. The total number of charm pairs as a function of the proper time τ is shown in the right window of Fig. 3. As shown by the dashed line, including only the leading-order contribution from two-body processes increases the number of charm pairs by about 10% during the evolution of the quark–gluon plasma, reaching a final value of about 22. Adding the next-leading-order contribution further increases the charm quark pair number by about 25% to about 27 as shown by the solid line. We have also found that thermal production of charm quarks from the quark–gluon plasma becomes more important as the initial number of charm quark pairs is smaller, *e.g.*, the final numbers are about 19, 27, and 45, respectively, for initial numbers of charm quark pairs of 10, 20 and 40. The number of charm quark pairs produced from the quark–gluon plasma would be reduced by a factor of about 3 if a larger charm quark mass of 1.5 GeV or a lower initial temperature of $T_0 = 630$ MeV is used. The latter corresponds to an initial energy density similar to those predicted by the AMPT model [26] and the Color Glass Condensate [27], although both have considerable uncertainties. Thermal charm quark production is, however, not much affected if gluons and quarks are taken to be massless due to increase in their densities. On the other hand, increasing the initial temperature to 750 MeV would enhance the thermally produced charm quark pairs by about a factor of 2. Using a larger quark–gluon formation time of $\tau_0 = 0.5\ {\rm fm}/c$ reduces the initial temperature of the quark–gluon plasma but not much the final number of charm quark pairs.

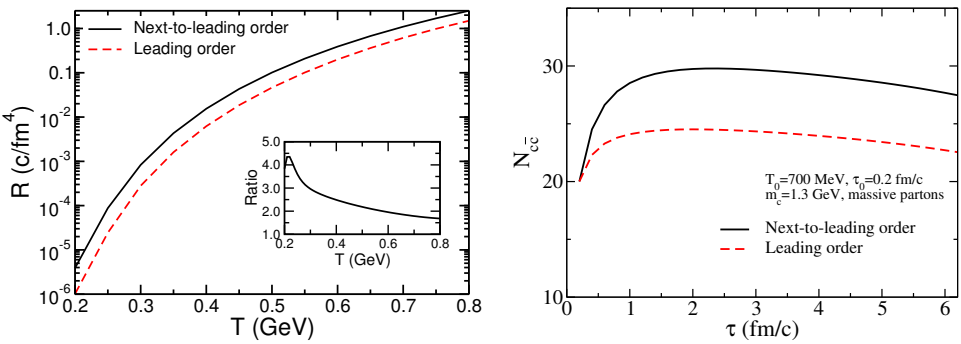

Fig. 3. (Color online) Left window: Charm quark production rate per unit volume as a function of temperature. The inset gives the ratio between charm production rates in the next-to-leading and the leading order. Right window: Time evolution of charm quark pair numbers in central Pb + Pb collisions at $\sqrt{s_{NN}} = 5.5$ TeV.

5. Charmed multiquark hadron production

Possible enhancement of charm quark production from the quark–gluon plasma formed in heavy-ion collisions at LHC provides the opportunity to search for exotic charmed multiquark hadrons that might be formed during the hadronization of the quark–gluon plasma. Possible existence of stable multiquark hadrons that consist of heavy quarks can be understood in terms of arguments based on the simplified form of the color–spin interaction [28], $C_H \sum_{i>j} \vec{s}_i \cdot \vec{s}_j / m_i m_j$, where m and $\vec{s}$ are the mass and spin of the constituent quarks i and j. The strength of the color–spin interaction C_H should depend on the wave function and the exact form of the interaction as well as the color structure of either the quark–quark or quark–antiquark pair. This simple form with $C_H = C_B$ for a diquark and $C_H = C_M$ for a quark–antiquark pair can capture some of the essential physics in hadron masses. With the constituent quark masses $m_{u,d} = 300$ MeV, $m_s = 500$ MeV, $m_c = 1500$ MeV, and $m_b = 4700$ MeV, the mass splittings between many hadrons and their spin flipped partners can be reasonably described with $C_B/m_u^2 = 193$ MeV and $C_M/m_u^2 = 635$ MeV. The mass difference between a tetraquark meson with identical diquarks $T_{q_1q_2}(ud\bar{q}_1\bar{q}_2)$ and the sum of vector meson $M^*(u\bar{q}_1)$ and pseudo scalar meson $M(d\bar{q}_2)$ masses due to the color–spin interaction is then given by $-\frac{3}{4}\frac{C_B}{m_u^2} + \frac{1}{4}\frac{C_B}{m_{q_1}^2} - \frac{1}{4}\frac{C_M}{m_u m_{q_1}} + \frac{3}{4}\frac{C_M}{m_u m_{q_1}}$. Since this mass difference decreases as q_1 and q_2 become heavy, tetraquark mesons $T_{cc}(ud\bar{c}\bar{c})$ and $T_{bb}(ud\bar{b}\bar{b})$ are bound by 79 MeV and 124 MeV, respectively. This is contrary to the tetraquark meson $T_{ss}(ud\bar{s}\bar{s})$, which is unbound by 63 MeV. Essentially the same results have been obtained in the full constituent quark model calculation [29, 30] and the QCD sum-rule calculation [31]. Similar considerations can be applied to tetraquark baryons $\Theta_{sq}(udus\bar{q})$. It is then found that the tetraquark baryon $\Theta_{sc}(udus\bar{c})$ is bounded relative to ND_s by 30 MeV and ΣD by 69 MeV, while it is unbound relative to ΛD by only 8 MeV. For the tetraquark baryon $\Theta_{sb}(udus\bar{b})$, it is bounded by 68, 133, and 56 MeV relative to NB_s, ΣB, and ΛB, respectively.

Using the quark coalescence model, we have estimated the yields of these exotic multiquark hadrons in heavy-ion collisions at both RHIC and LHC. Because of the expected large charm quark number in central Pb + Pb collisions at LHC, the abundance of the tetraquark meson T_{cc} and pentaquark baryon Θ_{cs} are about 10^{-4} and 10^{-3}, respectively. We have also discussed their decay modes to illustrate how they can be identified in heavy-ion collisions. In our studies, we have not taken into account the hadronic effect on the abundance of these charmed exotics, as hadronic reactions that affect their annihilation and production are unknown. Since the yields of T_{cc} and Θ_{cs} from the coalescence model is significantly smaller than those expected from the statistical hadronization model, including the hadronic effect is expected to increase their yields substantially and reduces the differences

from the predictions from the quark coalescence model and the statistical hadronization model. We thus expect that the open and hidden charmed hadron physics will be an interesting subject in the forthcoming heavy-ion collision experiments.

6. Summary

We have found that because of the high density in the QGP, charm energy loss due to three-body scattering becomes non-negligible. Including this effect helps explain the observed small nuclear modification factor of non-photonic electrons from heavy meson decays in these collisions. The formation of the QGP at RHIC also enhances significantly the production of charmed Λ_c relative to that of D^0, particularly if strong diquark correlations exist in the QGP. We have also shown that because of the high initial temperature that is expected to be achieved in the quark–gluon plasma produced in heavy-ion collisions at LHC, thermal charm quark production may be important. This provides the possibility to search for possible exotic charmed multiquark hadrons such as $T_{cc}(ud\bar{c}\bar{c})$ and $\Theta_{sc}(uds\bar{c})$. Verification of the existence of these exotic hadrons will open a new frontier in charmed hadron spectroscopy.

REFERENCES

[1] T. Matsui, H. Satz, *Phys. Lett.* **B178**, 416 (1986).

[2] G.D. Moore, D. Teaney, *Phys. Rev.* **C71**, 064904 (2005).

[3] V. Greco, C.M. Ko, R. Rapp, *Phys. Lett.* **B595**, 202 (2004).

[4] B. Zhang, L.W. Chen, C.M. Ko, *Phys. Rev.* **C72**, 024906 (2005); *Nucl. Phys.* **A774**, 665 (2006).

[5] L.W. Chen, C.M. Ko, W. Liu, M. Nielsen, *Phys. Rev.* **C76**, 014906 (2007).

[6] S.H. Lee, S. Yasui, W. Liu, C.M. Ko, *Eur. Phys. J.* **C54**, 259 (2008).

[7] C.M. Ko, W. Liu, *Nucl. Phys.* **A783**, 233c (2007); W. Liu, C.M. Ko, *J. Phys.* **G34**, S775 (2007).

[8] S.H. Lee, K. Ohnishi, S. Yasui, I.K. Yoo, C.M. Ko, *Phys. Rev. Lett.* **100**, 22301 (2008).

[9] Y. Oh, C.M. Ko, S.H. Lee, S. Yasui, *Phys. Rev.* **C79**, 044905 (2009).

[10] B.W. Zhang, C.M. Ko, W. Liu, *Phys. Rev.* **C77**, 024901 (2008).

[11] S.S. Alder *et al.* [PHENIX Collaboration], *Phys. Rev. Lett.* **96**, 032301 (2006).

[12] J. Bielcik, *Nucl. Phys.* **A774**, 697 (2006).

[13] M.G. Mustafa, *Phys. Rev.* **C72**, 014905 (2005).

[14] C. Wicks, W. Horowitz, M. Djordjevic, M. Gyulassy, *Nucl. Phys.* **A784**, 426 (2007).

[15] H. van Hees, R. Rapp, *Phys. Rev.* **C71**, 034907 (2005).

[16] A. Adil, I. Vitev, *Phys. Lett.* **B649**, 139 (2007).

[17] J. Adams *et al.* [STAR Collaboration], *Phys. Rev. Lett.* **94**, 062301 (2005).

[18] M. Cacciari, P. Nason, R. Vogt, *Phys. Rev. Lett.* **95**, 122001 (2005).

[19] D. Teaney, J. Lauret, E. Shuryak, *Phys. Rev. Lett.* **86**, 4783 (2001); P. Huovinen, P.F. Kolb, U. Heinz, *Nucl. Phys.* **A698**, 475 (2002); T. Hirano, K. Tsuda, *Phys. Rev.* **C66**, 054905 (2002).

[20] Z.W. Lin, C.M. Ko, *Phys. Rev.* **C65**, 034904 (2002); D. Molnar, M. Gyulassy, *Nucl. Phys.* **A697**, 495 (2002).

[21] O. Kaczmarek, F. Karsch, F. Zantow, *Phys. Rev.* **D70**, 074505 (2004).

[22] Y. Oh, C.M. Ko, *Phys. Rev.* **C79**, 067902 (2009).

[23] P. Levai, R. Vogt, *Phys. Rev.* **C56**, 2707 (1997).

[24] W. Beenakker *et al.*, *Phys. Rev.* **D40**, 54 (1989); W. Beenakker *et al.*, *Nucl. Phys.* **B351**, 507 (1991).

[25] P. Nason, S. Dawson, R.K. Ellis, *Nucl. Phys.* **B303**, 607 (1989); *Nucl. Phys.* **327**, 49 (1989).

[26] B. Zhang, C.M. Ko, Z.W. Lin, B.A. Li, *Phys. Rev.* **C61**, 067901 (2000); Z.W. Lin, S. Pal, C.M. Ko, B.A. Li, B. Zhang, *Phys. Rev.* **C64**, 011902(R) (2001); Z.W. Lin, C.M. Ko, B.A. Li, B. Zhang, S. Pal, *Phys. Rev.* **C72**, 064901 (2005).

[27] T. Lappi, *Phys. Lett.* **B643**, 11 (2006).

[28] A. De Rujula, H. Georgi, S.L. Glashow, *Phys. Rev.* **D12**, 147 (1975).

[29] S. Pepin *et al.*, *Phys. Lett.* **B393**, 119 (1997).

[30] B. Silvestre-Brac, C. Semay, *Z. Phys.* **C59**, 457 (1993).

[31] F.S. Navarra, M. Nielsen, S.H. Lee, *Phys. Lett.* **B649**, 166 (2007).